

# Graph Neural Network Flavor Tagger and measurement of $\sin 2\beta$ at Belle II

P. Stavroulakis on behalf of the Belle II collaboration  
*Université de Strasbourg, CNRS, IPHC UMR 7178, F-67000 Strasbourg, France*

We present GFaT, a new algorithm that uses a graph-neural-network to determine the flavor of neutral  $B$  mesons produced in  $\Upsilon(4S)$  decays. We evaluate its performance using  $B$  decays to flavor-specific hadronic final states reconstructed in a  $362 \text{ fb}^{-1}$  sample of electron-positron collisions recorded at the  $\Upsilon(4S)$  resonance with the Belle II detector at the SuperKEKB collider. We achieve an effective tagging efficiency of  $(37.40 \pm 0.43 \pm 0.36)\%$ , where the first uncertainty is statistical and the second systematic, which is 18% better than the previous Belle II algorithm. Demonstrating the algorithm, we use  $B^0 \rightarrow J/\psi K_S^0$  decays to measure the direct and mixing-induced  $CP$  violation parameters,  $C = (-0.035 \pm 0.026 \pm 0.013)$  and  $S = (0.724 \pm 0.035 \pm 0.014)$ , from which we obtain  $\beta = (23.2 \pm 1.5 \pm 0.6)^\circ$ .

## 1 Introduction

In the standard model of particle physics, an irreducible complex phase in the Cabibbo-Kobayashi-Maskawa (CKM) matrix<sup>1</sup> gives rise to  $CP$  violation. Measurements of mixing-induced  $CP$  violation in  $B^0$  meson decays constrain the values of the CKM-unitarity-triangle angles  $\beta$  and  $\alpha$ <sup>a</sup>, which helps probe for sources of  $CP$  violation beyond the standard model. Such measurements require knowledge of the neutral  $B$  meson flavor. At Belle II<sup>2</sup>,  $B^0$  and  $\bar{B}^0$  mesons are produced in coherent pairs from  $e^+e^-$  collisions at the  $\Upsilon(4S)$  resonance. Since they are entangled, tagging the flavor of one of the mesons,  $B_{\text{tag}}$ , at the time of its decay determines the flavor of the other one,  $B_{\text{sig}}$ , at that same time<sup>3</sup>. The probability density to observe  $B_{\text{sig}}$  decay to a  $CP$  eigenstate at a time  $\Delta t$  from when  $B_{\text{tag}}$  decays with flavor  $q_{\text{tag}}$  (+1 for  $B^0$ , -1 for  $\bar{B}^0$ ) is given by

$$P(\Delta t, q_{\text{tag}}) = \frac{e^{-|\Delta t|/\tau}}{4\tau} \{1 + q_{\text{tag}}(1 - 2w)[S \sin(\Delta m_d \Delta t) - C \cos(\Delta m_d \Delta t)]\}, \quad (1)$$

where  $q_{\text{tag}}$  is determined by the flavor tagger,  $w$  is the probability to wrongly determine it,  $\tau$  is the  $B^0$  lifetime, and  $\Delta m_d$  is the difference of masses of the  $B^0$  mass eigenstates<sup>4</sup>. Here  $S$  and  $C$  are parameters that quantify mixing-induced and direct  $CP$  violation. In the standard model,  $S = \sin 2\beta$  and  $C = 0$  to good precision<sup>5,6</sup>.

In order to be able to measure  $S$  and  $C$  as accurately as possible, one needs to have precise knowledge of  $w$ . We determine it from events where  $B_{\text{sig}}$  decays to  $B^0 \rightarrow D^{(*)-} \pi^+$ , for which

$$P(\Delta t, q_{\text{sig}}, q_{\text{tag}}) = \frac{e^{-|\Delta t|/\tau}}{4\tau} \{1 - q_{\text{sig}}q_{\text{tag}}(1 - 2w) \cos(\Delta m_d \Delta t)\}, \quad (2)$$

Besides flavor tagging effects, the finite resolution of the detector also affects the determination of  $\Delta t$  and therefore all time-dependent measurements. We account for this by convolving Eq. 1 and 2 with the  $\Delta t$  resolution model used in Ref<sup>4</sup>.

<sup>a</sup>These angles are also known as  $\phi_1$  and  $\phi_2$ .

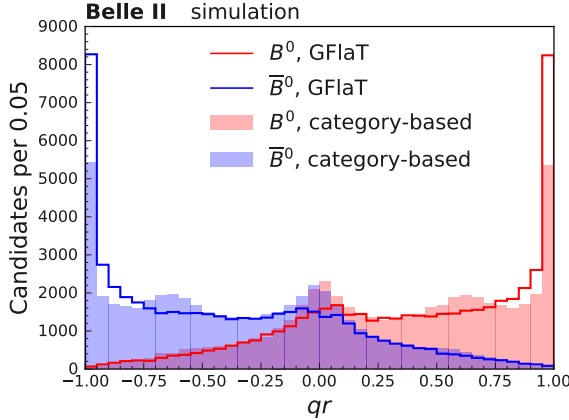


Figure 1 – Distributions of  $qr$  for true  $B^0$  and  $\bar{B}^0$  from GFlaT and the category-based flavor tagger in simulated data.

## 2 Flavor Tagging at Belle II

### 2.1 Category-based Flavor Tagger

Until recently, flavor tagging was performed at Belle II via a category-based approach<sup>7</sup> which uses topological, kinematic and particle identification information from the decay of the  $B_{\text{tag}}$  in order to assign it to one of several flavor-specific tagging categories. The assignment with the highest probability is then used to make a prediction on the flavor of  $B_{\text{tag}}$ , exploiting the correlation between the charge of one of the final state particles and the flavor of the decaying  $B$  meson. The output of this category-based flavor tagger consists of the flavor of  $B_{\text{tag}}$  at the time of its decay,  $q_{\text{tag}}$ , and the confidence of the flavor assignment,  $r$ , which can range anywhere between 0 (lowest confidence) to 1 (highest confidence).

The mistag probability,  $w$ , is characteristic of the flavor tagger and is usually determined in seven bins of  $r$  defined by the edges  $[0.0, 0.1, 0.25, 0.45, 0.6, 0.725, 0.875, 1.0]$ . To evaluate the performance of the flavor tagger we use the effective tagging efficiency,

$$\varepsilon_{\text{tag}} = \sum_i \varepsilon_i (1 - 2w_i)^2, \quad (3)$$

where  $\varepsilon_i$  is the efficiency to assign a flavor to  $B_{\text{tag}}$  and  $w_i$  is the mistag probability in the  $i$ -th  $r$  bin. A higher effective tagging efficiency directly translates to more statistically precise measurements of  $S$  and  $C$ .

### 2.2 Graph-Neural-Network Flavor Tagger

Recently, a new flavor tagging algorithm<sup>8</sup> based on a dynamic-graph-convolutional neural network<sup>9</sup> was developed at Belle II, which makes use of the relational information between the final state particles in the tag-side in order to increase the effective tagging efficiency.

Figure 1 shows the  $qr$  distributions of both the category-based and graph-neural-network-based flavor taggers. The latter improves on the former via better tagging of events in which the  $B_{\text{tag}}$  decays into final states without any charged leptons. This leads to a  $qr$  distribution that is more peaking at the edges and flatter in the middle and, consequently, to a relative improvement of 20% in effective tagging efficiency, that is estimated from simulation.

## 3 Calibration of GFlaT

We use  $B^0 \rightarrow D^{(*)-} \pi^+$  decays to evaluate the performance of GFlaT and calibrate its parameters, since they allow to access the flavor of  $B_{\text{sig}}$  without the need for flavor tagging. To achieve this,

we perform a time-dependent analysis, that allows to also extract the parameters of the  $\Delta t$  resolution function.

We specifically reconstruct  $D^- \rightarrow K^+ \pi^- \pi^-$  decays and  $D^{*-} \rightarrow \bar{D}^0 \pi^-$  decays with  $\bar{D}^0 \rightarrow K^+ \pi^-$ ,  $K^+ \pi^- \pi^0$ , or  $K^+ \pi^- \pi^+ \pi^-$ , using charged particle tracks and calorimeter clusters.  $B^0$  candidates are reconstructed from a  $D^{(*)-}$  and a charged particle track consistent with a  $\pi^+$ . A kinematic fit is performed for each  $B^0$  candidate in order to determine its decay vertex position.

We first perform an unbinned maximum likelihood fit to the  $\Delta E$  distribution, defined as  $\Delta E \equiv E - E_{\text{beam}}$ , where  $E_{\text{beam}}$ ,  $E$  are the beam energy and  $B^0$  energy in the c.m. frame, respectively. We then subtract the background in the  $\Delta t$  distribution using  $sWeight$ <sup>10</sup> and fit the resulting signal distribution simultaneously in the 7 bins of  $r$ , 2 flavors of  $B_{\text{tag}}$  and 2 flavors of  $B_{\text{sig}}$  to extract the parameters of the flavor tagger and  $\Delta t$  resolution function. The parameters obtained with the procedure described above are considered<sup>b</sup> to be independent of decay mode and are used in all subsequent time-dependent measurements.

Figure 2 shows the signal extraction fit to the  $\Delta E$  distribution as well as the fit to the background-free  $\Delta t$  distribution in the  $r$ -bin with the highest confidence. We obtain an effective tagging efficiency of

$$\varepsilon_{\text{tag}} = (37.40 \pm 0.43 \pm 0.36)\%$$

For comparison, we evaluate the effective tagging efficiency using the category-based flavor tagger on the same set of data and obtain  $\varepsilon_{\text{tag}} = (31.68 \pm 0.45)\%$ . Therefore, we conclude that GFlaT yields a relative improvement of 18% in effective tagging efficiency over the category-based flavor tagger.

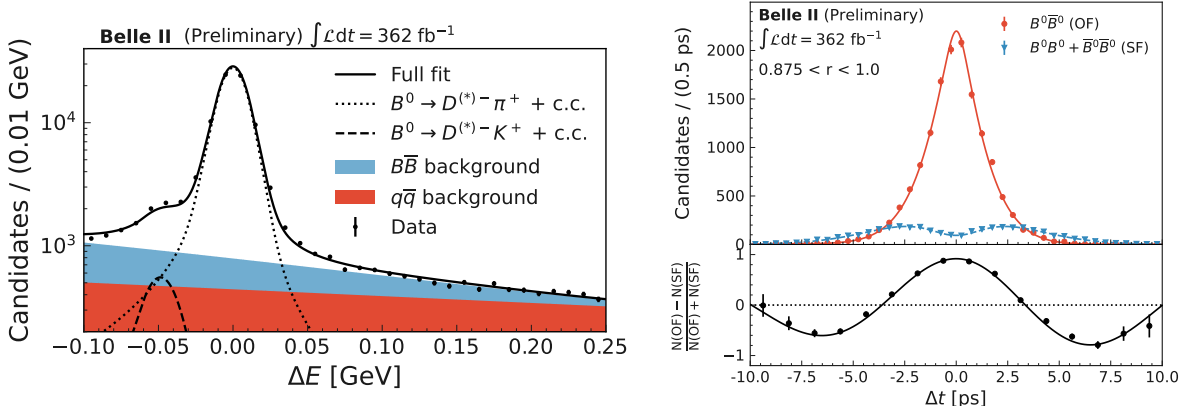


Figure 2 – Distributions of  $\Delta E$  (left) and background-subtracted  $\Delta t$  (right) distributions in the seventh  $r$ -bin for  $B^0 \rightarrow D^{(*)-} \pi^+$  (points) and the best-fit functions (lines). The background components of the fit to the  $\Delta E$  distribution are stacked.

#### 4 Measurement of $\sin 2\beta$ using GFlaT

We validated GFlaT through a measurement of  $S$  and  $C$  in  $B^0 \rightarrow J/\psi K_S^0$  decays. We reconstruct  $J/\psi$  candidates via  $J/\psi \rightarrow e^+ e^-$  or  $\mu^+ \mu^-$  and  $K_S^0$  candidates via  $K_S^0 \rightarrow \pi^+ \pi^-$ .

A signal extraction fit is performed on the  $\Delta E$  distribution, from which  $sWeights$  are computed and then used to subtract the background in the  $\Delta t$  distribution. We then fit the resulting  $\Delta t$  distribution simultaneously in the 7 bins of  $r$  and 2  $B_{\text{tag}}$  flavors to extract  $S$  and  $C$ . For this fit, we use the  $\Delta t$  resolution model and flavor tagging parameters that were calibrated using  $B^0 \rightarrow D^{(*)-} \pi^+$  decays. The fit procedure is validated using  $B^0 \rightarrow J/\psi K^{*0}$  decays, where

<sup>b</sup>This assumption was verified between  $B^0 \rightarrow D^{(*)-} \pi^+$  and  $B^0 \rightarrow J/\psi K_S^0$  decays in simulation.

both  $S$  and  $C$  are expected to be zero. Figure 3 shows the fits to the  $\Delta E$  and background-subtracted  $\Delta t$  distributions in events containing  $B^0 \rightarrow J/\psi K_S^0$  decays. We obtain

$$S = 0.724 \pm 0.035 \pm 0.014, \\ C = -0.035 \pm 0.026 \pm 0.013,$$

The statistical uncertainties are 8% and 7% smaller, respectively, than they would be if measured using the category-based flavor tagger, which is expected given the higher effective tagging efficiency of GFlaT. From  $S$ , we calculate  $\beta = (23.2 \pm 1.5 \pm 0.6)^\circ$ <sup>c</sup>, which agrees with previous measurements by *BABAR*<sup>12</sup>, *Belle*<sup>13</sup> and *LHCb*<sup>14</sup>.

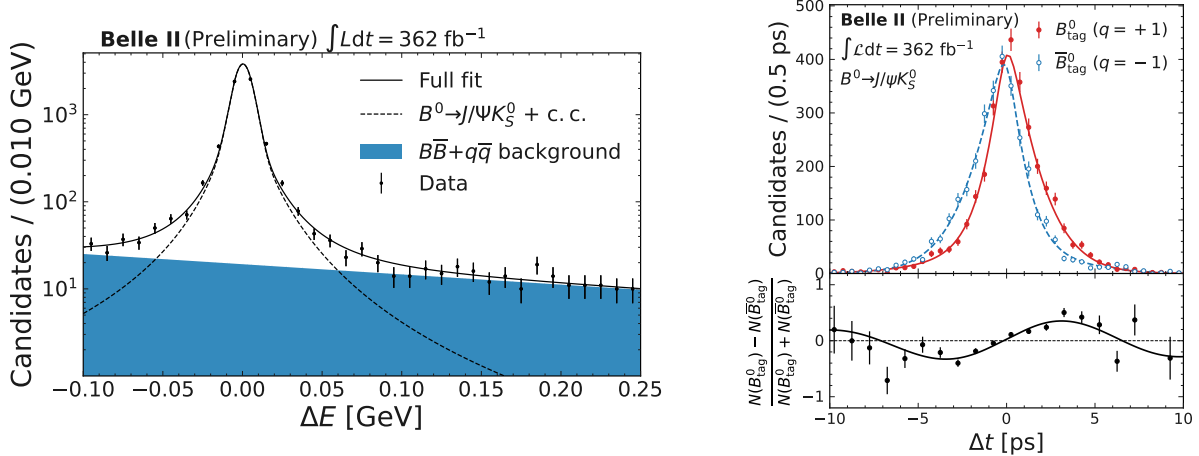


Figure 3 – Distributions of  $\Delta E$  (left) and background-subtracted  $\Delta t$  (right) distributions in the full  $r$  range for  $B^0 \rightarrow J/\psi K_S^0$  (points) and the best-fit functions (lines).

## References

1. M. Kobayashi and T. Maskawa, *Prog. Theor. Phys.* **49**, 652 (1973).
2. T. Abe et al. (Belle II Collaboration), arXiv:physics/1011.0352.
3. I. I. Y. Bigi and A. I. Sanda, *Nucl. Phys. B* **193**, 85-108 (1981).
4. F. Abudinén et al. (Belle II Collaboration), *Phys. Rev. D* **107**, 091102 (2023).
5. K. De Bruyn and R. Fleischer, *JHEP* **03**, 145 (2015).
6. M. Barel and K. De Bruyn and R. Fleischer and E. Malami, *J. Phys. G* **48**, 065002 (2021).
7. F. Abudinén et al. (Belle II Collaboration), *Eur. Phys. J. C* **82**, 283 (2022).
8. I. Adachi et al. (Belle II Collaboration), arXiv:physics/2402.17260.
9. H. Qu and L. Gouskos, *Phys. Rev. D* **101**, 056019 (2020).
10. M. Pivk and F. Le Diberder, *Nucl. Instrum. Methods A* **555**, 356-369 (2005).
11. A. Abdesselam et al. (BABAR Collaboration), *Phys. Rev. Lett.* **115**, 121604 (2015).
12. B. Aubert et al. (BABAR Collaboration), *Phys. Rev. D* **79**, 072009 (2009).
13. I. Adachi et al. (Belle II Collaboration), *Phys. Rev. Lett.* **108**, 171802 (2012).
14. R. Aaij et al. (LHCb Collaboration), *Phys. Rev. Lett.* **132**, 021801 (2024).

<sup>c</sup>The other solution  $\pi/2 - \beta$  is excluded from independent measurements<sup>11</sup>